A Model for Analyzing the Performance of Wireless Multi-Hop Networks using a Contention-based CSMA/CA Strategy

Sajid M. Sheikh[1*], Riaan Wolhuter[2] and Herman A. Engelbrecht[3]
[1,2,3] Department of Electrical and Electronic Engineering, University of Stellenbosch,
Private Bag X1, Matieland, Stellenbosch 7602, South Africa
[e-mail: sajid.sheikh@mopipi.ub.bw,wolhuter@sun.ac.za, hebrecht@sun.ac.za]
*Corresponding author: Sajid M. Sheikh

Received October 21, 2016; revised January 10, 2017; revised February 21, 2017; accepted March 18, 2017; published May 31, 2017

Abstract

Multi-hop networks are a low-setup-cost solution for enlarging an area of network coverage through multi-hop routing. Carrier sense multiple access with collision avoidance (CSMA/CA) is frequently used in multi-hop networks. Multi-hop networks face multiple problems, such as a rise in contention for the medium, and packet loss under heavy-load, saturated conditions, which consumes more bandwidth due to re-transmissions. The number of re-transmissions carried out in a multi-hop network plays a major role in the achievable quality of service (QoS). This paper presents a statistical, analytical model for the end-to-end delay of contention-based medium access control (MAC) strategies. These strategies schedule a packet before performing the back-off contention for both differentiated heterogeneous data and homogeneous data under saturation conditions. The analytical model is an application of Markov chain theory and queuing theory. The M/M/1 model is used to derive access queue waiting times, and an absorbing Markov chain is used to determine the expected number of re-transmissions in a multi-hop scenario. This is then used to calculate the expected end-to-end delay. The prediction by the proposed model is compared to the simulation results, and shows close correlation for the different test cases with different arrival rates.

Keywords: Queue Model, Markov Model, End-to-end Delay, Scheduling, Absorbing state, CSMA/CA

https://doi.org/10.3837/tiis.2017.05.011 **ISSN : 1976-7277**

1. Introduction

The IEEE 802.11 standard was designed for wireless connectivity in single-hop networks and has been in use for over a decade. This standard has also found numerous applications in multi-hop networks, and has become the predominant standard in the field of networking [1,2].

Multi-hop networks face multiple challenges. These include a drop in throughput as the number of hops to reach the destination increases; an increase in contention for the channel; and starvation issues for heterogeneous data under loads where data starts to queue up in a node using the enhanced distributed channel access (EDCA) scheduling technique [1,2]. Starvation refers to lower-priority data packets gaining less access to the channel for transmission compared to high-priority data. Our approach has been to develop schedule-before-contention (SBC) strategies, which has led to the model presented here. Existing SBC strategies such as congestion control and fairness scheduling (CCFS) [3], adaptive weighted round-robin scheduling [4], Schedule Before Backoff (SBB) [5], and random priority-based scheduling [6] have been shown to cause a reduction in packet loss, a reduction in collisions, and an improvement in fairness for heterogeneous data in multi-hop networks.

CSMA/CA has two access techniques, namely a basic mechanism and a Request-to-Send/Clear-to-Send (RTS/CTS) access mechanism. With the basic mechanism, the transmitter sends a packet, and the receiver acknowledges receipt of the packet by sending an acknowledgement (ACK) message. With RTS/CTS, the channel is reserved before transmission. In this paper, we present a novel model to predict the queuing delay for data of different priority levels within a node. We also present a novel Markov chain model to determine the expected number of re-transmissions for CSMA/CA,using the basic access mechanism in a multi-hop network for SBC approaches. The number of re-transmissions plays a critical role in the achievable end-to-end delay in multi-hop networks. To the best of our knowledge, this is the first analytical model to use this approach.

The end-to-end delay model is made up of the waiting time as well as the service time at each hop to reach the destination. The model to calculate the end-to-end delay consists of three sub-models. First, an absorbing-state Markov chain model is developed to determine the expected number of re-transmissions at each hop. Secondly, the access delay model is derived. Lastly, we derive the expected end-to-end delay by using the values obtained from the expected re-transmissions and access delay models. This analytical model is applicable to modeling of general strategies that first select a packet for transmission and then perform back-off contention in multi-hop networks. Examples of these strategies are the basic distributed coordination function (DCF) access mechanism, which does not differentiate between data, and data-differentiated strategies such as random weighted scheduling (RWS), as we proposed in[6]. The model is tested with both DCF and RWS. First-order Markov models operate from the philosophy that the performance of the current state does not depend on the history of the previous states, and can only be used for scheduling strategies whose operation do not depend on history. The proposed model conforms to the concept of a Markov model.

In recent studies, CSMA/CA has been applied to LTE-unlicensed (LTE-U) systems to share access to the unlicensed spectrum [7]. In multi-hop networks using CSMA/CA, a channel bandwidth of 20MHz is used for every transmission, while with LTE, nodes can transmit using different spectrum bandwidths, ranging from 1.4MHz to 20MHz. The MAC layer of LTE uses orthogonal frequency division multiple access (OFDMA), which splits the

available bandwidth into multiple sub-carriers. Therefore, the bandwidth for CSMA/CA in LTE is shared by multiple users, while in multi-hop networks the bandwidth can only be used by a single user at a time. IEEE 802.11-based multi-hop networks that use CSMA/CA experience more interference than LTE-U networks [7].The model in this paper is applicable to CSMA/CA as used in multi-hop networks with single-radio, single-channel (SRSC) technologies.

The rest of this paper is organized as follows. In Section 2, the related work is presented. Section 3 gives a brief overview of an absorbing-state Markov chain model. Section 4 presents the assumptions made during the modeling process, as well as the networks that were used to obtain the results. Section 5 contains the end-to-end delay analytical model for both single-queue and multi-queue strategies. Section 6 describes the model itself and the simulation parameters used. The simulation and analytical results are presented in Section 7 and Section 8offers conclusions.

2. Related Work

The Bianchi model proposed for the distributed coordination function (DCF) was one of the first analytical models to predict the performance in CSMA/CA[8]. This model computes the IEEE 802.11 DCF throughput by making assumptions of all nodes within the transmission range for a single-hop network under ideal channel conditions. The model also considers the RTS/CTS access mechanisms [8]. This model proposes a Markov chain approach to model the binary back-off process.

Over the last decade, the Bianchi model has become the foundation for many other models, such as analytical models for the priority-based EDCA strategy [9–13]. Most of these models can be classified into one of two categories, namely saturation or non-saturation load conditions. By saturation, we mean that the node always has a packet to send, and by non-saturation that the node does not always have a packet to send. In Bianchi's model, the countdown timer for the back-off does not stop when the channel becomes busy. In [10], Xiao extends the work of Bianchi to develop a model to analyze the contention window size differentiation for the different priority queues in EDCA, but assumes equal arbitration inter-frame spacing (AIFS) periods for all traffic classes. In [9], an analytical model for EDCA throughput is proposed which considers collision probabilities for both saturation and non-saturation cases, with and without using a virtual collision handler (VCH). In [11], the performance of EDCA is analyzed based on both AIFS and retry limits for the contention window range, building on the work of [10]. In [12], expressions for the non-saturation throughput in EDCA are developed. In [14], an analytical model for both the saturated and non-saturated throughput, the end-to-end delay and the frame-dropping probabilities of the different traffic classes is proposed. In [13], a saturation throughput model is developed.

In [15], the authors propose a model to analyze the throughput of EDCA in multi-hop networks. The model does not compare the analytical results with any simulations or testbed implementation results. The work takes into account non-saturation traffic conditions and hidden node problems by separating the problem into two models, based on a Markov chain. One model is for the node, and the other is for the channel conditions. In [16], an analytical model for queuing delay in EDCA is analyzed for single-hop scenarios.

A three-dimensional Markov chain model for the back-off operation is proposed in [17]. The authors derive the throughput for saturation conditions and do not consider the virtual collision mechanism.The authors in [18] also propose a three-dimensional Markov chain

model for the back-off operation for single-hop networks. Their model is an extension of Bianchi's model for saturated and non-saturated traffic. Other models that calculate the saturated throughput by extending Bianchi's model in single-hop networks include [18–20] and [11]. Non-saturated throughput is calculated in the work by [12]. A novel, high-performance EDCA approach called H-EDCA to partition the collision domain of different classes of traffic based on Bianchi's model is proposed in [22]. Anapproach other than using the Markov chain is applied by the authors in [23], by using hierarchical stochastic activity networks (HSAN), which employ a stochastic Petri network to calculate the throughput. The work in [24]is an extension of Xiao's model and as such uses Markov chains to model the back-off mechanism. Its authors consider not only saturated traffic, but also non-saturated traffic for throughput and delay calculations. They furthermore consider access delay in their model.

A mean values analysis approach is used in [25] to calculate the saturated throughput for single-hop networks. The model considers the change of the CW size and AIFS. A model for collision probability, throughput and access delay for both saturated and non-saturated delay in single-hop networks based on Bianchi's model is proposed in [26] for EDCA. There, the authors use Pareto optimal pairs for the number of stations and for different parameter sets and loads. A survey of DCF and EDCA models applied to single-hop networks is presented in [27].

All of the models discussed so far have been applicable to single-hop networks only. Most of the Markov models are discrete-time Markov chain (DTMC) models. The bi-dimensional Markov model has become a frequently used tool for analyzingperformance in CSMA/CA considering back-off duration. The majority of the existing body of work focuses on calculating the throughput and the mean delay by considering only the delay on the medium, and not the queuing time in the node. Numerous models exist which are designed and applied to single-hop networks,but not multi-hop networks.

Interference plays a significant role in performance in multi-hop networks, as shown in [28], [29], [30] and [31], as the carrier-sensing range exceeds the transmission range in cases of overlapping collision domains [29]. A problem that is known as adjacent channel interference (ACI) exists in multi-hop networks, where "bleeding over" can take place. ACI causes sensing from outside of a node's transmission range. Therefore, whenever a node within the interference range transmits, all other nodes within this range have to wait [30]. This is also called co-channel interference, and will lead to a node's neighbours using the same channel as if they were within interference range of each other, thereby affecting the capacity of the network [31]. Most existing models also do not consider the re-transmission limit in their approach, and do not calculate the estimated number of transmissions that take place.

In summary, the aspects not covered by existing work are multi-hop networks with re-transmission calculations, access delay, and capacity degradation with an increase in the number of nodes in the network. The advantage of our proposed model is that it does consider these values in multi-hop networks.

3. Absorbing-State Markov Chain Modeling

We use an absorbing-state Markov chain model to predict the expected number of re-transmissions at each hop in a network. In this section, we present a brief overview of Markov chain theory. A Markov chain is a popular stochastic model used to model dynamic systems that change their states over time. They can be classified as either a discrete-time

Markov chain (DTMC) or a continuous-time Markov chain (CTMC) [32].

A stochastic process $\{ X_n \}$, with discrete time $n \in N = \{ 0, 1, 2, \ldots \}$ and a discrete set of possible states for the system, is known as a DTMC. X_n presents the state of the chain at n. Markov chains possess the Markov property, which states that the behaviour of the next state depends only on the state the system is in at present, and not its past states [32,33].

In a Markov chain, a state can transit to the next state at time n. A Markov chain is known to be absorbing if it has an absorbing state such that once this state is entered, the model cannot exit this state. An essential feature of absorbing Markov chains (AMC) is that eventually an absorbing state is entered [32,34].

To solve absorbing Markov chains, the following steps are taken [34]:

a) The transition matrix is written in standard form. P is the transition matrix of a DTMC such that p_{st} is the probability of a transition from state s to state t. For an absorbing Markov chain, all the absorbing states are written such that they precede the non-absorbing states. The canonical-form matrix P is given as:

$$P = \begin{array}{c} \\ \text{Absorbing} \\ \text{Non-absorbing} \end{array} \begin{array}{c} \begin{array}{cc} \text{Absorbing} & \text{Non - absorbing} \end{array} \\ \begin{bmatrix} I & 0 \\ R & Q \end{bmatrix} \end{array}$$

P now has four sub-matrices, where:

- I is a square identity matrix of size equal to the number of absorbing states for the number of rows and also the number of absorbing states for the number of columns.
- 0 is a rectangular zero matrix of size equal to the number of absorbing states for the number of rows and the number of non-absorbing states for the number of columns.
- R is the rectangular matrix of transition probability from a non-absorbing state to an absorbing state of size equal to the number of non-absorbing states for the number of rows and the number of absorbing states for the number of columns.
- Q is a square matrix of transition probability from a non-absorbing state to a non-absorbing state of size equal to the number of non-absorbing states for the number of rows and also the number of non-absorbing states for the number of columns.

b) To determine the limiting matrix steady state (or the long-term behaviour of an absorbing Markov chain), we multiple P by itself continuously.

$$P^2 = \begin{bmatrix} I & 0 \\ R & Q \end{bmatrix} \begin{bmatrix} I & 0 \\ R & Q \end{bmatrix} = \begin{bmatrix} I & 0 \\ R+QR & Q^2 \end{bmatrix}$$

$$P^3 = \begin{bmatrix} I & 0 \\ R+QR & Q^2 \end{bmatrix} \begin{bmatrix} I & 0 \\ R & Q \end{bmatrix} = \begin{bmatrix} I & 0 \\ R+QR+Q^2R & Q^3 \end{bmatrix}$$

$$P^t = \begin{bmatrix} I & 0 \\ (I+Q+Q^2+\ldots\ldots+Q^{t-1})R & Q^t \end{bmatrix}$$

As $t \to \infty$ then $Q^t \to 0$. The limiting matrix form that has now been obtained, has the form:

$$\overline{P} = \begin{array}{c} \\ \text{Absorbing} \\ \text{Non - absorbing} \end{array} \begin{array}{c} \begin{array}{cc} \text{Absorbing} & \text{Non - absorbing} \end{array} \\ \begin{bmatrix} I & 0 \\ FR & 0 \end{bmatrix} \end{array}$$

The system will move to some absorbing state. The limiting matrix is a simplified notation of multiplying P with itself until infinity. The fundamental matrix (F) is calculated as:

$$F = (I - Q)^{-1} \quad (3)$$

To determine the limiting matrix, FR must be calculated and then written in the form above.

c) The number of steps that it takes to reach the absorbing node is calculated by summing each row in the fundamental matrix (F) to give the expected number of periods (t) spent in each non-absorbing state before reaching the absorbing state. The sum of each row can easily be derived by multiplying the F matrix with a column matrix whose entries are all 1.

$$t = Fc \quad (4)$$

where c is a column matrix whose entries are all 1.

d) The following equation is used to determine the probability of entering an absorbing state given the current state.

$$B = FR \quad (5)$$

$B_{y,z}$ is the probability of being absorbed in the absorbing state z from a transient state y. In B, $y$is the row elements representing the non-absorbing states, and $z$is the column elements representing the absorbing states.

4. Assumptions and Network

This section presents the assumptions made in order to develop the analytical model, as well as the multi-hop networks used for the testing of the model and to obtain the results in Section 8.

A node is made up of arriving packets, packets being serviced and packets queued.

The following assumptions are made:

1. The packets for the different priority classes are of equal length. In telemetry networks, packet sizes are usually between 60 bytes and 600 bytes [35-37]. Smaller packets have a lower probability of collision, as they are less prone to collisions [38]. Therefore, in this model, packet size is not taken into account.
2. The arrival rate is assumed to be a random Poisson distribution, as the arrival events occur independently.
3. Each queue in each node follows the M/M/1 queuing principles, as the arrival rates are assumed to follow a Poisson process and the departure rates are assumed to have an exponential distribution.(If the waiting time is unknown, it is appropriate to model the system with an exponential distribution.)Both of these distributions are memory-less and thus we use the M/M/1 queue model. The number 1 is used because we use a single channel for transmission.

4. The optional RTS/CTS mechanism in the IEEE 802.11 standard is not used, as the mechanism under study is the basic mechanism.
5. The channel is in ideal conditions. This is to say that the model assumes there are no channel errors, no capture effects and no hidden terminal problems.
6. All nodes are in saturation. This is to say that it is assumed that every node always has data available in its buffer to transmit.
7. The system is slotted. This is to say that a node is only allowed to send data at the beginning of the time slot. The countdown for the back-off takes place in discrete time step intervals equal to the time slot. This condition makes it possible to model the system as a DTMC model.
8. The collision probability is constant for a given traffic load, depending on the network size and priority data class.
9. The queuing system is open, meaning packets can enter and leave the queue in a node.
10. The data priority queues in each node have infinite length, and no packets are dropped due to congestion.
11. The transmission opportunity (TXOP) limit is not used. If TXOP bursting is used, where multiple packets can be transmitted when the node gains access to the channel, the queue resembles a G/G/1 queuing system and the M/M/1 equations will not hold.

In this model, only the important aspects of the MAC layer scheduling strategies are modeled, while the parts that are not under study are simplified or omitted. The important aspects are the scheduling strategy operation, the queue waiting time, and collisions. Theexcluded parts are information about other layers, such as the application, transport, network and physical layers and their overheads.

Different multi-hop network sizes (from a one-hop network size to a five-hop network size, as shown in **Fig. 1**) are used to obtain the results in the analysis of the model presented in the next section. A maximum network size of five is used for two reasons, the first being that it is rare to have wireless multi-hop networks with data having to be transmitted over a large number of hops. (The model is, however, applicable to bigger networks as well.)Secondly, the model holds under stability conditions; a large number of hops for transmission would make the system unstable. A stable system is one where the arrival rate is less than the departure rate,where the queue length is finite, and where dropping of packets from the queue does not take place due to capacity. The stability of a system depends on the transmission rates, arrival rate, and packet size.

The transmission range for each node is shown as dotted lines in **Fig. 1**. The interference range is greater than the transmission range, as the strategy uses SRSC technology [29]. Another node within the interference range that wants to send data will detect the channel as being busy if a transmission is taking place by a node within the transmission range. The source node sendsthe data to the destination node for the different network sizes, as shown in **Fig. 1**; all the intermediate nodes only forward the data. The distance between the nodes has an effect on the propagation delay to transmit packets between nodes, as well as on the bit error rate (BER). The transmission range of each node in a network is such that only one-hop transmission can take place.

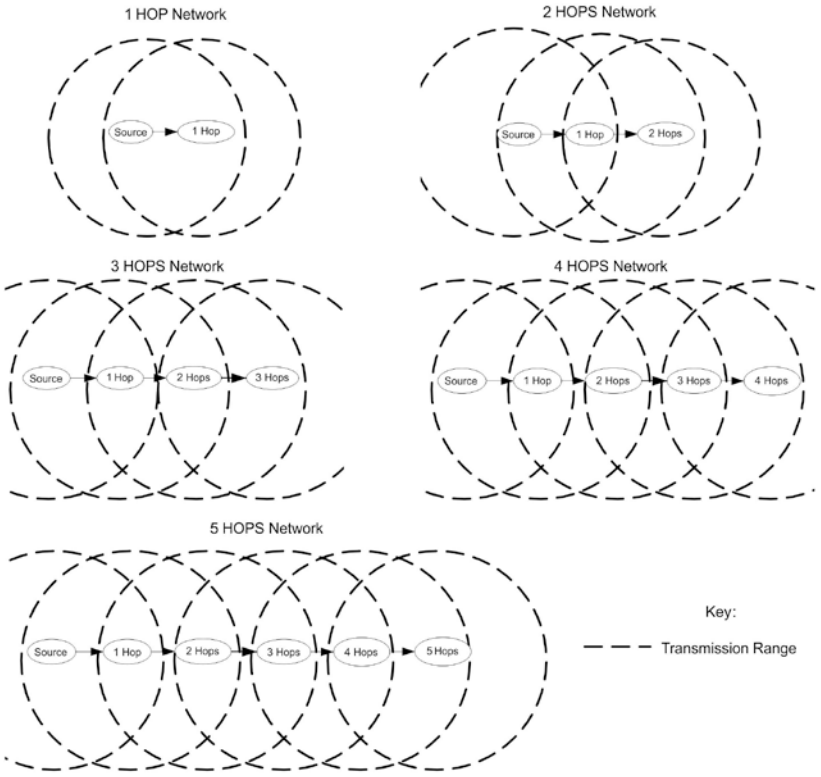

Fig. 1. The multi-hop networks under study

5. End-to-End Delay Analytical Model

End-to-end delay is defined as the time that elapses from the time the packet is sent to the time that it successfully reaches its destination. The end-to-end delay is the total of all the waiting times in the queue and service times at each hop link for a packet to reach the destination from the source node. In other words, the true sojourn time is the sum of the basic access times and the queuing times at each node at each hop. The waiting times at each node are made up of the access delay time; the arbitration inter-frame spacing (AIFS) for a multi-queue system or DCF inter-frame spacing (DIFS) for a single-queue system; and the back-off time, which depends on the contention window (CW) size. The service time on each link is made up of the time to transmit the header of the packet, the time to transmit the payload of the packet, the short inter-frame spacing (SIFS) period, the time to transmit the acknowledgement (ACK) message, the propagation delay, the ACK-timeout period in the event that no ACK is received, and the number of transmissions at each hop link. These parameters are illustrated in **Fig. 2** for each hop link. The medium access delay equations are also presented in [39], [9] and [12].

In this section, we develop a model to calculate the end-to-end delay for a single-queue SBC strategy such as DCF, as well as for a multi-queue SBC strategy such as RWS.

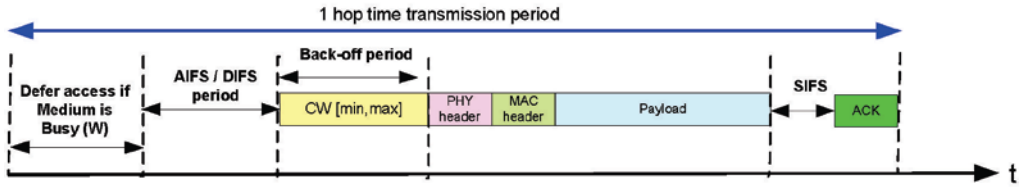

Fig. 2. Timing diagram for sojourn time at each hop link

5.1 Single-Queue Strategy

DCF uses a single queue in each node, with data treated on a first in, first out (FIFO) basis. With DCF, the end-to-end delay for a successful transmission on the h^{th} hop link (TS_h) is given by:

$$TS_h = DIFS + BO + SIFS + ACK + W_h + PropDelay + \frac{L}{R_t} \quad (6)$$

where *DIFS* is the DIFS duration; *SIFS* is the SIFS time period; *ACK* is the time it takes to transmit back an acknowledgement; W_h is the access delay time at the h^{th} hop; *PropDelay* is the propagation delay time which is the time taken to transmit a signal based on the distance between the nodes; L is the size of the packet including the header and payload; BO is the back-off duration, which depends on the CW value selected; and R_t is the average transmission rate on the medium.

If a collision takes place, the collision time is expressed as:

$$TC = DIFS + BO + SIFS + ACK_{TIMEOUT} + PropDelay + \frac{L}{R_t} \quad (7)$$

$$ACK_{TIMEOUT} = SIFS + ACK + PropDelay \quad (8)$$

Equations 7 and 8 are derived from the fact that if a node does not receive an acknowledgment from the receiver within a time period of $ACK_{TIMEOUT}$, the sender assumes that a collision occurred, or that the packet did not reach its destination successfully. Therefore, another transmission attempt is made. The collision time in Equation 7 therefore also includes the additional $ACK_{TIMEOUT}$ period before attempting another transmission attempt.

The end-to-end delay (D) over all the hop links includes the successful transmission time on each hop link, the collision time, and the number of re-transmissions, and is expressed as:

$$D = \sum_{h=1}^{H} (TS_h + NR_h * TC) \quad (9)$$

where NR_h is the number of re-transmissions at the h^{th} hop link and H is the maximum number of hop links from the source to the destination.

In Section 5.1.1,we will now explain how the expected number of re-transmissions at each hop is calculated. Section 5.1.2 explains how the access delay time is calculated,and Section 5.1.3 shows how the stability of the system is calculated.

5.1.1 Expected Number of Re-transmissions

To calculate the expected number of re-transmissions in a multi-hop path network, we modeled the system as an absorbing-state DTMC. The notation used to represent the states is*hop number, transmission number*. Since a maximum of seven re-transmissions is allowed by the 802.11 protocol, the eighth transmission attempt represents an unsuccessful transmission of a packet where the packet is dropped [40,41]. States 1,8; 2,8; 3,8 … up to *N*,8 and the destination state are all made absorbing states. *N*,8 is the state that is entered at the N^{th} hop number and after the seventh transmission attempt. A transition to the next hop node depends on the probability of success on the channel. A transition to the next transmission attempt state at the same hop node depends on the probability of not being successful. An *N*-hop network is shown in **Fig. 3**.

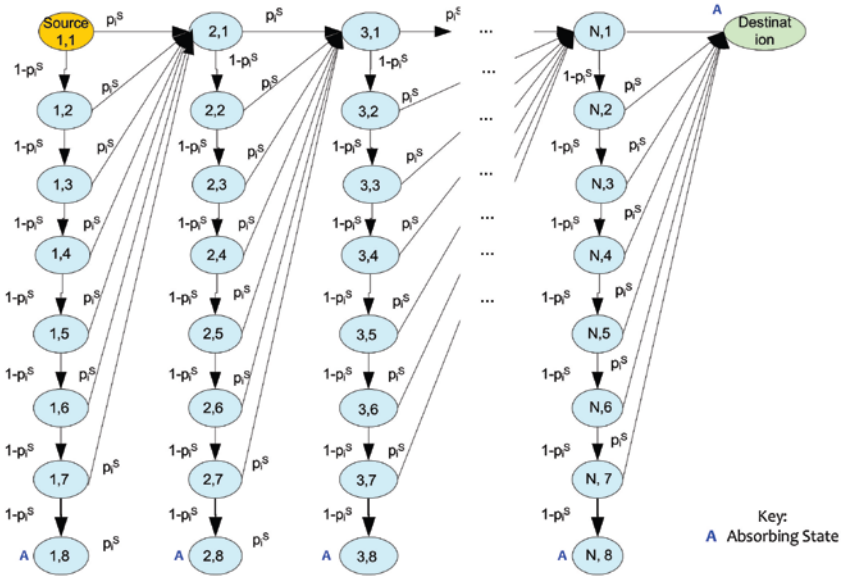

Fig. 3. The absorbing Markov chain model for a multi-hop network

Limiting matrices for the different network sizes are derived. For a one-hop network, the transition matrix (written in standard form, as explained in Section 3, with the absorbing states written ahead of the non-absorbing states) is:

$$\overline{P}_{1hopnetwork} = \begin{array}{c} \\ \text{Absorbing states} \\ \text{Non-absorbing states} \end{array} \begin{array}{c} \begin{array}{cccccccccc} & \text{Absorbing states} & & \multicolumn{7}{c}{\text{Non-absorbing states}} \\ & 1,8 & \textit{Destination} & 1,1 & 1,2 & 1,3 & 1,4 & 1,5 & 1,6 & 1,7 \end{array} \\ \begin{array}{c} 1,8 \\ \textit{Destination} \\ 1,1 \\ 1,2 \\ 1,3 \\ 1,4 \\ 1,5 \\ 1,6 \\ 1,7 \end{array} \begin{pmatrix} 1 & 0 & 0 & 0 & 0 & 0 & 0 & 0 & 0 \\ 0 & 1 & 0 & 0 & 0 & 0 & 0 & 0 & 0 \\ 0 & P_s & 0 & 1-P_s & 0 & 0 & 0 & 0 & 0 \\ 0 & P_s & 0 & 0 & 1-P_s & 0 & 0 & 0 & 0 \\ 0 & P_s & 0 & 0 & 0 & 1-P_s & 0 & 0 & 0 \\ 0 & P_s & 0 & 0 & 0 & 0 & 1-P_s & 0 & 0 \\ 0 & P_s & 0 & 0 & 0 & 0 & 0 & 1-P_s & 0 \\ 0 & P_s & 0 & 0 & 0 & 0 & 0 & 0 & 1-P_s \\ 1-P_s & P_s & 0 & 0 & 0 & 0 & 0 & 0 & 0 \end{pmatrix} \end{array}$$

These matrices are then used to determine the expected number of transmissions between each hop to reach the destination with the application of Equation 4 (the number of steps that it takes to reach the absorbing node). The probability of reaching a certain absorbing state is calculated using Equation 5 (the probability that, if a system is in a particular state, it will reach the absorbed state).

To determine the probability of successful transmission on the channel (a value needed in the limiting matrices), we first derive the probabilities for collision on the channel, andthe probability of error on the channel. We then use these probabilities to calculate the probability of successful transmission on the channel.

The probabilities are estimated as follows:

a) Probability of collision on the channel: The probability of collision in a time slot is dependent on the transmission attempt probability and the number of nodes that cannot transmit while any one of the other nodes is transmitting. The probability of collision is calculated based on the fact that a collision takes place when one node transmits and any of the *N*-1 remaining nodes also transmits a packet in the same time slot. The transmission attempt probability of a node is inversely proportional to its contention window size under saturation [35–39]. The value of CW is selected as $CW_{\min}$ when the first collision takes place. The probability of collision negates multiple re-transmissions, as the probability of success that is needed in the model is based on the first attempt, and onetransmission attempt is statistically independent of others.

The transmission attemptprobability (τ) can be expressed as:

$$\tau = \frac{1}{CW_{\min}} \tag{11}$$

The system is backlogged if the queue is not empty, as stated in [47]. The transmission attempt probability increases with an increase in load. This happens as a result of queues with data countdown, when achannel is detected as being idle and then freezes when a transmission takes place. With a higher load, there is a higher chance of more packets already having counted down for the back-off, and thus anincreased transmission attempt probability.This can be taken care of in the denominator, taking the arrival and departure rates of the nodes in the transmission range. For networks with nodes in the interference range, “bleeding” and overlapping of transmission ranges cause nodes that are trying to transmit to hear other communications beyond the transmission range. This happens if SRSC technology is used and all nodes are configured to the same channel frequency. A signal with significant power in one region can cause a node’s neighbours to detect the strong signal and thus prevent them from transmitting. This causes their transmission to be delayed even further. The number of nodes within the interference range that prevents concurrent transmission depends on the size of the network. The new transmission attempt probability,considering the load and the nodes in the interference range, now becomes:

$$\tau = \frac{1}{(CW_{\min})(1-\rho)} \tag{12}$$

where

$$\rho = \frac{\lambda}{\mu} \tag{13}$$

The simplified derived equation for collision probability within a time slot now becomes:

$$P_c = 1-(1-\tau)^{N-1} \tag{14}$$

The system holds for the following conditions:

$$0 \le \rho < 1$$

$$0 \le \tau < 1$$

where N is the number of nodes in the interference range, ρ is the traffic density (also known as the utilization factor), μ is the departure rate, and λ is the arrival rate.

b) Probability of error in transmission: Bit error rate (BER) plays a significant role in the successful receiving of a packet. Packets with errors have to be re-transmitted, and packet size has a great impact on the performance of the system. Larger packet size will result in higher packet errors. The probability of error is calculated based on BER and packet length (L) as:

$$P_{error} = 1 - (1 - BER)^{L} \quad (15)$$

We assume ideal channel conditions, and therefore $BER = 0$.

c) Probability of successful transmission: The overall probability of successful transmission over the channel is calculated as:

$$P_s = 1 - P_c - P_{error} \quad (16)$$

The calculated probability of successful transmission is used for the absorbing Markov chain model presented in **Fig. 3**. Equation 4 is used to determine the expected number of transmissions between each hop to reach the destination.

d) Average CW size: We calculate the average back-off CW size as in [48]. The probability of collision in the channel is P_c, and the probability of no collision is $1\text{-}P_c$. The $CW_{\min}$ value is doubled each time a collision occurs. These factors are used in a renewal reward process to calculate the approximate average back-off CW as a geometric distribution, summing the results up to the first success and considering re-transmissions:

$$CW_{avgbackoff} = (1-P_c)\frac{CW_{min}}{2} + P_c(1-P_c)\frac{2CW_{min}}{2} + \ldots + P_c^{M}(1-P_c)\frac{2^{M}CW_{min}}{2} + P_c^{M+1}\frac{2^{M}CW_{min}}{2} \quad (17)$$

where M is the maximum allowed exponential increase for the CW size, and $CW_{\min}$ is the minimum CW range size value. This equation gives us the expected number of CW back-off re-transmission sizes between renewal events. With a probability of $1\text{-}P_c$, the transmission is successful and the random number that is generated is assumed to be the mid-value between 0 and CW_{min}. The second term in the equation is when the first transmission fails and the second is successful. The contention window increases in size as well. The rest of the terms allow for up to M re-transmissions.

The obtained value for the number of transmissions can also be verified by calculating the average CW size using Equation 17, and determining the range into which this value falls. $CW_{\min}$ is incremented exponentially after every collision until it reaches $CW_{\max}$. After it reaches $CW_{\max}$, it stays constant until a successful transmission, or until the packet is dropped on reaching the maximum re-transmission limit.

5.1.2 Access Delay Time

The queue in a node with DCF is assumed to follow the principles of an M/M/1 queue. In [49], the DCF model in multi-hop networks also models the queues in a node using an M/M/1 queue. (In [50], EDCA is modeled as M/M/1.) The queue in a node with DCF is an M/M/1 queue because the arrival rate follows a Poisson distribution, with a fixed arrival rate for constant bit rate (CBR) data, and because the events occur independently; the departure rate is exponential, as the waiting time between events is unknown and random; and the system has one channel for the service of packets. The departures from one node feed into

the next nodeas arrivals. The access delay time (*W*), which is the time a packet waits in the queue, is derived in [51] as:

$$W = \frac{\rho}{\mu - \lambda} \tag{18}$$

5.1.3. Determining Network Stability

The number of packets in the node system gives a good indication of whether or not the system is in saturation. The number of packets in the system for an M/M/1 system can be calculated as [51]:

$$Pkt_s = \frac{\rho}{1-\rho} \tag{19}$$

The utilization equation presented in Equation 13 indicates the stability of a system. If the utilization is below 1, the system is known to be stable. If the calculated value is greater than 1, the system becomes unstable [51]. To determine if the system will be stable for the evaluated arrival rate for different network sizes, the utilization can be calculated considering each link in the interference range of the network under study.

5.2. Multi-Queue Strategy

In section 5.1 we derived the end-to-end model for a single-queue multi-hop system. In this section, we derive a model for a multi-queue system, using the RWS scheduling strategy. Thedata packets for each priority are of equal size. The system is a non-preemptive queuing system. For a preemptive queuing system, the ongoing service is halted when higher-priority data arrives. For a non-pre-emptive system, the ongoing service is not halted even if higher-priority data arrives.

With RWS, the end-to-end delay for a successful transmission on the h^{th} hop link for the j^{th} priority class (j = 1,2,…, J, where 1 representsthe highest-priority queue and J represents the lowest-priority queue) is given by:

$$TS_{j,h} = AIFS(j) + BO(j) + SIFS + ACK + W_{j,h} + PropDelay + \frac{L}{R_j} \tag{20}$$

where AIFS(j) is the AIFS duration for the j^{th} priority class; $W_{j,h}$ is the access delay time at the h^{th} hop for the j^{th} priority class; $BO(j)$ is the back-off duration for the j^{th} priority class; and R_j is the average transmission rate for priority class on the medium.

If a collision takes place, the collision time is expressed as:

$$TC(j) = AIFS(j) + BO(j) + SIFS + ACK_{TIMEOUT} + PropDelay + \frac{L}{R_j} \tag{21}$$

The end-to-end delay for the j^{th} priority queue (D_j) over all the hop links takes into account the successful transmission time on each hop link, the collision time, and the number of re-transmissions.

$$D_j = \sum_{h=1}^{H} (TS_{j,h} + NR_{j,h} * TC(j)) \tag{22}$$

where $NR_{j,h}$ is the number of re-transmissions at the h^{th} hop link for the j^{th} priority class.

To calculate the expected number of re-transmissions at each hop for each priority class, the same AMC model as in Section 5.1.1 is used, except that equations are derived to consider multiple queues, as explained in Section 5.2.1. Section 5.2.2 explains how the access delay time in RWS for each priority queue is calculated.

5.2.1 Channel Probabilities using Multi-Queue

The collision probability on the channel under conditions of stability, considering possible collisions due to packets from any of the priority classes from any of the other nodes, is derived from Equation 14 as:

$$P_c = 1 - \prod_{j=1}^{J} (1 - \tau_j)^{N-1} \tag{23}$$

where τ_j is the transmission probability of the j^{th} priority class data.

The probability of the channel being idle for a network with multi-class priority queues becomes:

$$P_{idle} = \prod_{j=1}^{J} (1 - \tau_j)^{N} \tag{24}$$

The probability of successful transmission is calculated as in Equation 16.

5.2.2 Access Delay using Multi-Queue

In a multi-queue system with J priority classes (j = 1,2,…, J), the arrival rates of the different classes are $\lambda_1, \lambda_2, \ldots, \lambda_J$. The mean and second moment of the service time of the different classes are $\overline{x_j}$ and $\overline{x_j^2}$ respectively. In this work, the derived mean results of the Pollaczek-Khinchine type for an M/G/1 priority system is used and extended to convert the system to M/M/1, as per the rule in [51]. The data packets from the different queues are served in the order in which they arrive at the particular queue.

In [51], the M/G/1 non-preemptive priority queuing model is presented. The model is simplified in our work to transmit data according to the assigned transmission probabilities from the different queues for the RWS scheduling strategy. The M/G/1 model is not suitable for our system, as the departure rate in our system is assumed to follow an exponential distribution for a discrete probability distribution that assumes an estimated output probability scheduling from each queue in the scenario when the system is saturated. The departures from the current hop node feed as input into the next hop node, and the arrival rates are totally independent. In the M/G/1 model, the residual service time is therefore modified to become exponential, and the service time is assumed to be exponential, since the next queue for packet transmission is chosen randomly, with fixed rates. This changes the system to become an M/M/1 non-preemptive priority system, as stated by the rules in [52] and [51]. An M/G/1 model is a semi-Markovian queuing system, and is solved with techniques like imbedded Markov chain and residual service time. The imbedded process looks at queue behavior at service completion, while the residual service time method models the system from an arriving packet's perspective.

The work in this model is based on the M/G/1 model using residual service time. The M/G/1 model is changed to an M/M/1 by changing the second moment to become $2\mu^{-2}$ for residual service time, according to the rules stated in [52] and [51].

The data packets are served by the same channel, with a general service time distribution with a mean $\overline{x_j}$ and second moment $\overline{x_j{}^2}$ for data packets belonging to class j. Equations 25 to 30are from [51]. A brief explanation of how waiting time is derived is then given before we develop our access queuing delay model.

The total packet arrival rate for all different priorities of data is:

$$\lambda = \sum_{j=1}^{J} \lambda_j \tag{25}$$

The utilization of data packets from class *j* is given by:

$$\rho_j = \lambda \bar{x}_j \tag{26}$$

The average system service time and utilization become:

$$\bar{x} = \sum_{j=1}^{J} \frac{\lambda_j}{\lambda} \bar{x}_j \tag{27}$$

$$\rho = \sum_{j=1}^{J} \rho_j \tag{28}$$

The mean residual service time (*R*) is the weighted sum of all the residual service times for each priority class, calculated in [51] as:

$$R = \sum_{j=1}^{J} \rho_j \left(\frac{\bar{x}_j^{2}}{2\bar{x}_j}\right) \tag{29}$$

The waiting time for a data packet of the n^{th} priority queue class that arrives at any of the different priority queues is made up of the mean residual service time, the total service times of the data packets already in the same priority queue, as well as the service time while other queues are being serviced. The derived waiting time is:

$$W_n = \frac{R}{(1-\rho_1-\rho_2-\ldots-\rho_{n-1})(1-\rho_1-\rho_2-\ldots-\rho_n)} \tag{30}$$

Using the theory in [51], it is stated that if the service time is exponential, then the second moment becomes $2\mu_j{}^{-2}$ for residual service time. Substituting this condition into Equation 29, the new residual service time makes the model M/M/1. The new value of *R* now becomes:

$$R = \sum_{j=1}^{J} \lambda_j \bar{x}_j^{2} \tag{31}$$

Combining Equations 30 and 31, we get the access delay time for the n^{th} priority queue in a node as:

$$W_n = \frac{\sum_{j=1}^{J} \lambda_j \bar{x}_j^{2}}{(1-\sum_{j=1}^{n-1} \rho_j)(1-\sum_{j=1}^{n} \rho_j)} \tag{32}$$

The access delay for the n^{th} priority queue at the h^{th} hop node can be written as:

$$W_{n,h} = \frac{\sum_{j=1}^{J} \lambda_{j,h} \overline{x}_{j,h}^{-2}}{(1-\sum_{j=1}^{n-1} \rho_{j,h})(1-\sum_{j=1}^{n} \rho_{j,h})} \qquad (33)$$

The channel utilization for the j^{th} class at the h^{th} hop node can be written as:

$$\rho_{j,h} = \lambda_{j,h} \overline{x}_{j,h} \qquad (34)$$

With the RWS scheduling strategy, a priority queue for a packet transmission is first chosen. This is done by assigning weights to each priority queue, after which a random number is generated. A priority queue into which the number falls is chosen to transmit a packet. A packet is selected, and then the contention periods of AIFS and back-off are carried out. The analysis network model is shown in **Fig. 1**. Each node receives and forwards data to the destination node, as shown in **Fig. 4**.

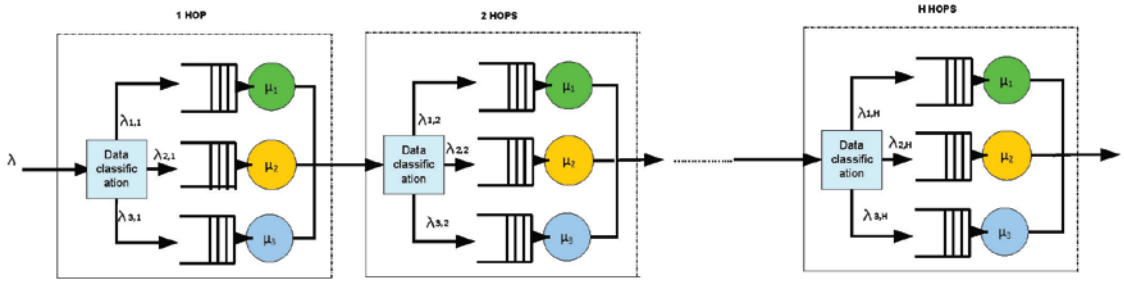

Fig. 4. A multi-hop network using the RWS scheduling strategy

The arrival rate for the j^{th} priority class at the h^{th} hop for the network under study in saturation can be expressed as:

$$\lambda_{j,h} = \lambda_h P W_j^{h-1} \qquad (35)$$

where PW_j is the scheduling weights assigned to the priority class in the RWS strategy.

Substituting Equations 34 and 35 into Equation 33, the access delay time in the queue for each priority queue at each hop node is derived.

$$W_{n,h} = \frac{\sum_{j=1}^{J} \overline{x_{j,h}^2} \lambda_h P W_j^{h-1}}{(1-\sum_{j=1}^{n-1} \overline{x_{j,h}} \lambda_{j,h})(1-\sum_{j=1}^{n} \overline{x_{j,h}} \lambda_{j,h})} \qquad (36)$$

6. Model Verification

To confirm the accuracy of our model, we compare the prediction of the analytical model to the simulation results obtained with OMNeT++. DCF has one queue in each node. For RWS, we implement three queues in each node. The parameters used in the simulations and the model are shown in **Table 1** and **Table 2** respectively. The results presented in this paper are for different load scenarios using DCF and RWS, as shown in **Table 3**.

Table 1. IEEE802.11g parameter values used

Parameter	Value
Simulation Time	900 sec
Path Loss Model	free space
Slot Time	9µsec
Channel Data Bit Rate	54Mbps
SIFS	10µsec
Basic Bit Rate	6Mbps
Propagation Delay	1µsec
PHY Preamble and Header	192 bits
MAC Header	272 bits
ACK	112 bits
Packet Size	512 bytes

Each node is configured with the IEEE 802.11g standard using 54Mbps as the data rate and 6Mbps as the basic rate. Acknowledgments are sent back at the basic rate, and this is also the rate at which packets leave the node for a queuing system if it is the only node contending for the medium. Each simulation is run five times, with different seed numbers for each run, and the average values were used for the results. The maximum and minimum values obtained from the different seed runs were used to plot the simulation error bars. To obtain the numerical results of the model, the equations were setup as functions in MATLAB.

Table 2. Default DCF and RWS strategy parameters used

	RWS Scheduling			DCF Scheduling
	High Priority (HP) Data	Medium Priority (MP) Data	Low Priority (LP) Data	
CWmin	7	15	31	31
CWmax	15	31	1023	1023
Retry Limit	7	7	7	7

Table 3. Test cases for different schedule-before-contention strategies

	Scheduling Strategy	Data Classes	Data Rates (packets per second)	Total Traffic (packets per second)	Network Utilization for Different Network Sizes				
					1 Hop	2 Hops	3 Hops	4 Hops	5 Hops
Scenario 1	DCF	1	200	200	0.136	0.273	0.41	0.55	0.682
Scenario 2	DCF	1	300	300	0.22	0.44	0.66	0.88	**1.10**
Scenario 3	RWS	3 (HP, MP and LP)	50	150	0.11	0.22	0.33	0.44	0.55
Scenario 4	RWS	3 (HP, MP and LP)	100	300	0.22	0.44	0.66	0.88	**1.10**
Scenario 5	RWS	3 (HP, MP and LP)	150	450	0.33	0.66	0.99	**1.33**	**1.66**

7. Results

This section presents the end-to-end delay for both ouranalytical model and the simulations. Our model and the simulated end-to-end delay results for the test case scenarios over the different hop network sizes are presented in **Fig. 5** for DCF and in **Fig. 6** for three-queue RWS scheduling. The stability calculated for each network size and load is presented

in **Table 3**. As mentioned before, the model is only valid when the network is stable.

Close correlation with the predicted results is observed. For the DCF case with one queue, the system becomes unstable for network sizes of greater than four hops for aload of 300packets per seconds (pps). This is in accordancewith the network utilization of 1.1 (calculated using Equation 13),which is greater than 1; hence the system becomes unstable.

The same instability effect is observed for the RWS cases, with three queues for a data rate of 100pps for each queue after four hops. In Test Scenario 4,the 150pps case with RWS with a data rate of 150pps for a network size greater than three hops is also unstable. The error bars show the range into which the simulated results fall with the use of different seeds. It is observed that with end-to-end delay, there is a small error range for the simulated results.

There are slight differences between ourmodel's results and the simulated results for the end-to-end delay. In most cases, the simulated results are higher than the model's results. The percentage of absolute error between the modeledand simulated end-to-end delay results is calculated in **Table 4**. The errors are all less than 17%, with most being below 10%. Higher absolute errors are observed at one-hop and two-hop nodes,as these nodes are not in saturation. Lower absolute errors are observed when the nodes are in saturation. The difference between the model'sand the simulation's results can be explained as follows:

(1) The model does not take into account when two nodes from different collision domains transmit at the same time and a collision occurs.

(2) The mid-value of the minimun CW values isused for the back-off duration, and thisis just an approximation. The actual value could be moreor less than this value.

(3) The model does not consider the period for whichthe back-off freezes when another node is in communication.

(4) The model does not consider information from other layers such as the application, transport, network, and physical layers, and their overheads.

Collisions result in the need for re-transmissions, which increases the end-to-end delay, as the data then have to travel over multiple hops to reach its destination. The collision probability therefore plays a critical role in the achievable end-to-end delay. The number of collisions increases with an increase in arrival rate and with the size of the network for all priority data classes.

Table 4. Percentage of absolute error between the simulated and modeled results for the end-to-end delay

	Scheduling Strategy	**Data Classes**	**Data Rates (packets per second)**	**Percentage of Error for End-to-End Delay (%)**				
				1 Hop	**2 Hops**	**3 Hops**	**4 Hops**	**5 Hops**
Scenario 1	DCF	1	200	4.45	8.86	4.38	6.19	1.58
Scenario 2	DCF	1	300	4.76	6.92	2.88	5.8	
Scenario 3	RWS	3	50 HP	9.52	3.92	3.49	0.77	2.73
Scenario 3	RWS	3	50 MP	13.89	3.70	6.82	0.05	0.39
Scenario 3	RWS	3	50 LP	7.27	16.95	4.74	2.93	4.11
Scenario 4	RWS	3	100 HP	8.70	3.51	6.48	1.10	
Scenario 4	RWS	3	100 MP	8.33	2.77	4.61	4.62	
Scenario 4	RWS	3	100 LP	7.14	9.84	6.22	3.10	
Scenario 5	RWS	3	150 HP	12.00	7.69	5.71		
Scenario 5	RWS	3	150 MP	7.69	2.15	2.25		
Scenario 5	RWS	3	150 LP	10.71	2.36	6.87		

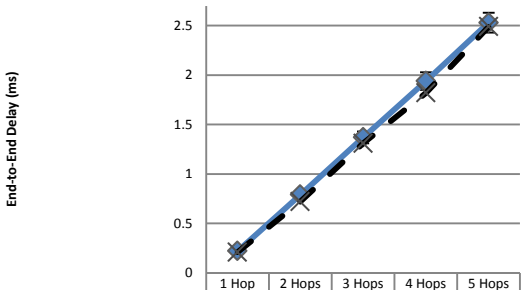

	1 Hop	2 Hops	3 Hops	4 Hops	5 Hops
Simulated Data	0.22	0.79	1.37	1.94	2.53
Analytical Model Data	0.21	0.72	1.31	1.82	2.49

200pps – Scenario 1

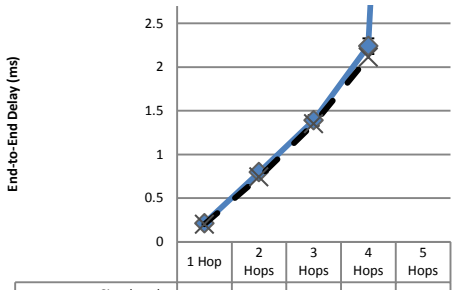

	1 Hop	2 Hops	3 Hops	4 Hops	5 Hops
Simulated Data	0.21	0.795	1.39	2.24	14.2
Analytical Model Data	0.2	0.74	1.35	2.11	

300pps - Scenario 2

Fig. 5. End-to-end delay with the DCF scenarios using homogeneous data

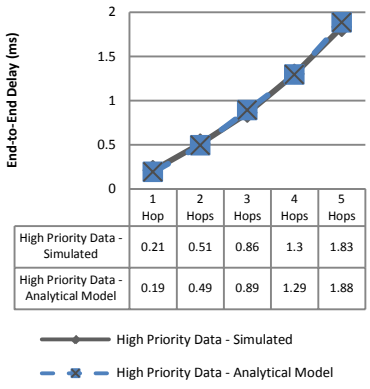

	1 Hop	2 Hops	3 Hops	4 Hops	5 Hops
High Priority Data - Simulated	0.21	0.51	0.86	1.3	1.83
High Priority Data - Analytical Model	0.19	0.49	0.89	1.29	1.88

High Priority Data - Simulated
High Priority Data - Analytical Model

(a) 50pps for High-Priority Data - Scenario 3

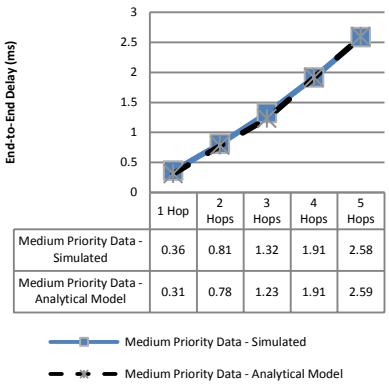

	1 Hop	2 Hops	3 Hops	4 Hops	5 Hops
Medium Priority Data - Simulated	0.36	0.81	1.32	1.91	2.58
Medium Priority Data - Analytical Model	0.31	0.78	1.23	1.91	2.59

Medium Priority Data - Simulated
Medium Priority Data - Analytical Model

(b) 50pps for Medium-Priority Data - Scenario 3

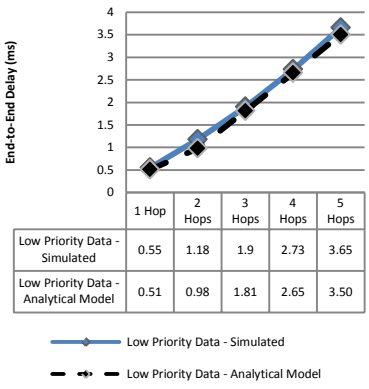

	1 Hop	2 Hops	3 Hops	4 Hops	5 Hops
Low Priority Data - Simulated	0.55	1.18	1.9	2.73	3.65
Low Priority Data - Analytical Model	0.51	0.98	1.81	2.65	3.50

Low Priority Data - Simulated
Low Priority Data - Analytical Model

(c) 50pps for Low-Priority Data - Scenario 3

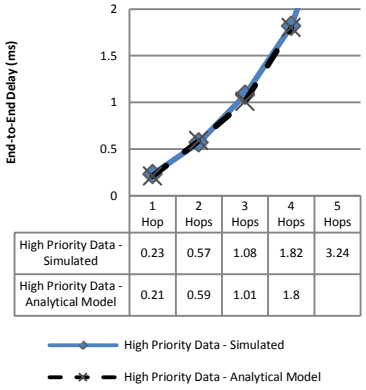

	1 Hop	2 Hops	3 Hops	4 Hops	5 Hops
High Priority Data - Simulated	0.23	0.57	1.08	1.82	3.24
High Priority Data - Analytical Model	0.21	0.59	1.01	1.8	

High Priority Data - Simulated
High Priority Data - Analytical Model

(d) 100pps for High-Priority Data - Scenario 4

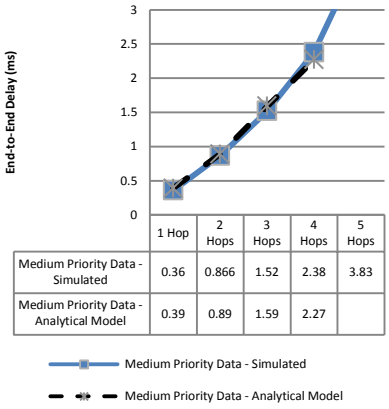

	1 Hop	2 Hops	3 Hops	4 Hops	5 Hops
Medium Priority Data - Simulated	0.36	0.866	1.52	2.38	3.83
Medium Priority Data - Analytical Model	0.39	0.89	1.59	2.27	

Medium Priority Data - Simulated
Medium Priority Data - Analytical Model

(e) 100pps for Medium-Priority Data - Scenario 4

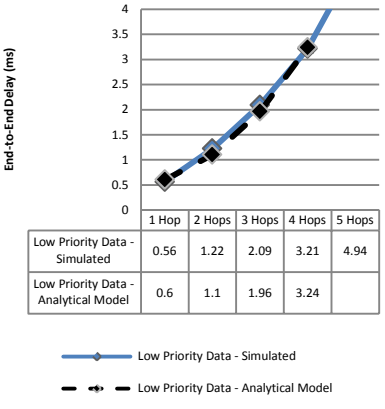

	1 Hop	2 Hops	3 Hops	4 Hops	5 Hops
Low Priority Data - Simulated	0.56	1.22	2.09	3.21	4.94
Low Priority Data - Analytical Model	0.6	1.1	1.96	3.24	

Low Priority Data - Simulated
Low Priority Data - Analytical Model

(f) 100pps for Low-Priority Data - Scenario 4

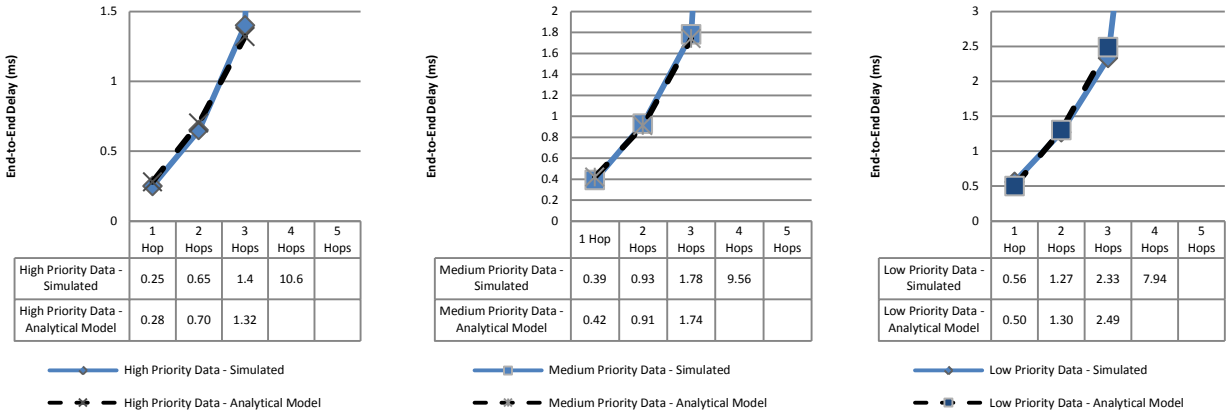

(g) 150pps for High-Priority Data - Scenario 5 (h) 150pps for Medium-Priority Data - Scenario 5 (i) 150pps for Low-Priority Data - Scenario 5

Fig. 6. End-to-end delay with three queue RWS scheduling scenarios using heterogeneous data

Conclusion

This paper presented a statistical, analytical model framework for the end-to-end delay calculations in a multi-hop network for schedule-before-contention MAC strategies. This model is applicable to networks with both single-queue and multiple-queue nodes for differentiated heterogeneous data. The model presented here applied Markov chain theory with absorbing states, as well as queuing theory. More specifically, M/M/1 queuing theory was used to represent the queues in a multi-hop network in order to derive the access queue waiting times.

The model is applicable to SRSC networks; therefore, the number of servers used in the queuing theory, was one. The arrival and departure rates from each queue were assumed to be Markovian. A Poisson random process of which the inter-arrival times are exponentially distributed was used to model the random arrival rates of the packets at each hop. An absorbing-state Markov chain model was developed to determine the expected number of re-transmissions with CSMA/CA between each hop in a multi-hop scenario. The absorbing states were employed when the seven-retry limit was exceeded at each hop, and the packet was discarded. Another absorbing state was that of the destination node.

Equations were derived to calculate the expected end-to-end delay by using the values obtained for the queue waiting time and the expected re-transmission models. In this model, the total end-to-end delay is made up of waiting times and system times. The waiting times at each hop node are made up of access delay time, AIFS or DIFS and back-off time, which depends on the contention window (CW) size. System time, in turn, is made up of the time to transmit the packet, the SIFS, the time to transmit the ACK message, the propagation delay, the ACK-timeout period in the event that no ACK is received, and the number of transmissions at each hop link. To use the Markov chain model that was developed here, the probability of successful transmission on the medium is required. This probability varies depending on the network size, the CW sizes, and the load level in the network.

In order to evaluate the accuracy of the proposed model, a comparison of the simulated and modeled end-to-end delay results was carried out by varying traffic loads for the different priority data classes. The results for the end-to-end delay model show close correlation, with an error percentage of less than 17% in the worst cases.

The model works for the basic channel access mechanism of CSMA/CA and excludes RTS/CTS. The overheads due to other layers are not considered. This model is designed for schedule-before-contention scheduling strategies in SRSC multi-hop networks. The number of re-transmissions plays a critical role in the end-to-end delay and reliability QoS that are achievable in multi-hop networks.

The model also indicates the collision probability expected in a multi-hop network. This model is important in view of the speed at which research and practice are moving towards using CSMA/CA in wireless multi-hop networks for extending networks or connecting different network clusters for applications such as smart grid, smart farming and smart health. In many of these networks, cost plays a significant role, and thus SRSC multi-hop network, with low-cost technologies will likely motivate more implementations. Collisions waste bandwidth, which is an important factor in determining the success of networks where bandwidth is limited. The availability of an analytical model could be useful in optimizing such networks.

References

[1] I. F. Akyildiz, X. Wang, and W. Wang, "Wireless mesh networks: a survey," *Comput. Networks*, vol. 47, no. 4, pp. 445–487, Mar. 2005. Article (CrossRef Link)

[2] P. H. Pathak and R. Dutta, "A Survey of Network Design Problems and Joint Design Approaches in Wireless Mesh Networks," *IEEE Commun. Surv. Tutorials*, vol. 13, no. 3, pp. 396–428, 2011. Article (CrossRef Link)

[3] S. M. Sheikh, R. Wolhuter, and H. A. Engelbrecht, "An Adaptive Congestion Control and Fairness Scheduling Strategy for Wireless Mesh Networks," in *Proc. of IEEE Symposium on Computational Intelligence for Communication Systems and Networks*, CIComms15, pp. 1174-1181, 2015. Article (CrossRef Link)

[4] S. M. Sheikh, R. Wolhuter, and G. J. Van Rooyen, "A Cross-Layer Adaptive Weighted Round Robin Scheduling Strategy for Wireless Mesh Networks," in *Proc. of Southern Africa Telecommunication Networks and Applications Conference* (SATNAC), pp. 323–328, 2015.

[5] S. Kuppa and R. Prakash, "Service differentiation mechanisms for IEEE 802.11 based wireless networks," *Wirel. Commun.* Netw. Conf., vol. 4, pp. 796–801, 2004. Article (CrossRef Link)

[6] S. M. Sheikh, R. Wolhuter, and H. A. Engelbrecht, "A Random Priority Based Scheduling Strategy for Wireless Sensor Networks Using Contiki," in *Proc. of International Conference on Wireless Information Networks and Systems* (WINSYS 2016), pp. 121-128, 2016. Article (CrossRef Link)

[7] T. Maksymyuk, M. Kyryk, and M. Jo, "Comprehensive Spectrum Management for Heterogeneous Networks in LTE-U," *IEEE Wirel. Commun.*, no. December, pp. 2–9, 2016. Article (CrossRef Link)

[8] G. Bianchi, "Performance Analysis of the IEEE 802.11 Distributed Coordination Function," *IEEE J. Sel. areas Commun.*, vol. 18, no. 3, pp. 535–547, 2000.

[9] R. Telenor, D. Unik, and O. N. Østerbø, "An Analytical Model of the Virtual Collision Handler of 802.11e," in *Proc. of* 8th ACM Int. Symp. Model. Anal. Simul. Wirel. Mob. Syst., pp. 255–259, 2004.

[10] Y. Xiao, "Performance analysis of priority schemes for IEEE 802.11 and IEEE 802.11e wireless LANs," *IEEE Trans. Wirel. Commun.*, vol. 4, no. 4, pp. 1506–1515, 2005. Article (CrossRef Link)

[11] I.-S. Hwang and H.-H. Chang, "Performance Assessment of IEEE 802.11e EDCF Using Three-dimension Markov Chain Model," Appl. Math. Sci., vol. 2, no. 3, pp. 139–151, 2008.

[12] G. Prakash and P. Thangaraj, "Analytical Modeling of IEEE 802.11e Enhanced Distributed Channel Access under a Non-Saturation Condition," *J. of Computer Science*, vol. 7, no. 4, pp. 554–560, 2011. Article (CrossRef Link)

[13] J. W. Robinson and T. S. Randhawa, "Saturation Throughput Analysis of IEEE 802.11e Enhanced Distributed Coordination Function," *IEEE J. Sel. Areas Commun.*, vol. 22, no. 5, pp. 917–928, 2004. Article (CrossRef Link)

[14] P. E. Engelstad and O. N. Osterbo, "Non-saturation and saturation analysis of IEEE 802.11e EDCA with starvation prediction," in *Proc. of 8th ACM Int. Symp. Model. Anal. Simul. Wirel. Mob. Syst.*, pp. 224–233, 2005. Article (CrossRef Link)

[15] M. T. Hoang, M. Hoang, and D. C. Le, "A Contribution to Performance Analysis Approach of the IEEE 802.11 EDCA in Wireless Multi-hop Networks," *VNU J. Sci. Comp. Sci. Com. Eng.*, vol. 31, no. 1, pp. 45–54, 2015

[16] P. Engelstad and O. Osterbo, "Queueing Delay Analysis of 802.11e EDCA," in *Proc. of Third Annu. Conf. Wirel. demand Netw. Syst. Serv.* (WONS 2006), pp. 123-133, 2006.

[17] Y. Lee, "Throughput Analysis Model for IEEE 802.11e EDCA with Multiple Access Categories," *J. Appl. Res. Technol.*, vol. 11, no. August, pp. 612–621, 2013. Article (CrossRef Link)

[18] B. Xie, J. Li, and L. Liu, "A Novel Performance Evaluation Model for IEEE 802.11e EDCA," *Adv. Sci. Technol. Lett.*, vol. 50, pp. 38–45, 2014. Article (CrossRef Link)

[19] D. Qiao and S. Choi, "Goodput enhancement of IEEE 802.11a wireless LAN via link adaptation," *IEEE Int. Conf. Commun.*, vol. 7, pp. 1995–2000, 2001.

[20] L. Bachiri, D. Aïssani, and L. Bouallouche-Medjkoune, "Saturation Throughput Analysis of the IEEE 802.11e EDCA Network with Contention Free Burst Under Fading Channel," *Wirel. Pers. Commun.*, vol. 79, no. 1, pp. 545–564, 2014. Article (CrossRef Link)

[21] N. C. Taher and E. Kobbeh, "A Complete and Accurate Analytical Model for 802.11e EDCA under Saturation Conditions," Syst. Res., pp. 800–807, 2009. Article (CrossRef Link)

[22] B. Chang, Y. Liang, and J. Chu, "Performance Analyses of High-Efficiency EDCA for Reducing Contention Collision and Increasing Throughput in QoS-based IEEE 802.11e Wireless Networks*," *J. Inf. Sci. Eng.*, pp. 1991–2007, 2010.

[23] S. Perez, H. Facchini, G. Mercado, L. Bisaro, and J. Campos, "EDCA 802.11e Performance under Different Scenarios: Quantitative Analysis," in *Proc. of 2013 IEEE 27th Int. Conf. Adv. Inf. Netw.* Appl., pp. 802–807, 2013. Article (CrossRef Link)

[24] P. E. Engelstad and O. N. Osterbo, "Queueing Delay Analysis of IEEE 802.11e EDCA," *Third Annual Conf. Wirel.* On-demand Netw. Syst. Serv., pp. 123–133, 2006.

[25] V. W. S. Wong, "Saturation throughput of IEEE 802.11e EDCA based on mean value analysis," IEEE Wirel. Commun. Netw. Conf. 2006. WCNC 2006., pp. 475–480, 2006.

[26] I. K. and V. A. Siris., "802.11e EDCA Protocol Parameterization : A Modeling and Optimization Study," Proc. IEEE Intl Symp. a World Wireless, Mob. Multimed. Networks, 2007

[27] K. Kosek-Szott, M. Natkaniec, and A. R. Pach, "A simple but accurate throughput model for IEEE 802.11 EDCA in saturation and non-saturation conditions," Comput. Networks, vol. 55, no. 3, pp. 622–635, 2011. Article (CrossRef Link)

[28] A. Busson and G. Chelius, A. Busson, "Capacity and interference modeling of CSMA/CA networks using SSI point processes," *Telecommun. Syst.*, vol. 57, no. 1, pp. 25–39, 2014. Article (CrossRef Link)

[29] Y. Shimoyamada, K. Sanada, N. Komuro, and H. Sekiya, "End-to-end throughput analysis for IEEE 802.11e EDCA string-topology wireless multi-hop networks," *Nonlinear Theory Its Appl. IEICE*, vol. 6, no. 3, pp. 410–432, 2015. Article (CrossRef Link)

[30] J. Nachtigall, A. Zubow, and J. P. Redlich, "The impact of adjacent channel interference in multi-radio systems using IEEE 802.11," in *Proc. of* IWCMC 2008 - Int. Wirel. Commun. Mob. Comput. Conf., pp. 874–881, 2008. Article (CrossRef Link)

[31] F. Bokhari and G. Záruba, "Partially Overlapping Channel Assignments in Wireless Mesh Networks," in *Proc. of Wireless Mesh Networks - Efficient Link Scheduling, Channel Assignment and Network Planning Strategies*, pp. 103–130, 2012.

[32] R. Weber, "Markov Chains," *Statslab.Cam.Ac.Uk*, pp. 28–49, 2012.
[33] O. Häggström, "Finite Markov chains and algorithmic applications," *London Math. Soc.*, vol. 52, 2002. Article (CrossRef Link)
[34] J. Montgomery, "04 Absorbing Markov Chains," Math. Model. Soc. Syst., no. February, pp. 1–14, 2009.
[35] M. H. Yaghmaee, M. Iran, Z. Yousefi, M. Zabihi, and S. Alishahi, "Quality of service guarantee in smart grid infrastructure communication using traffic classification," in *Proc. of International Conference on Electricity Distribution (CIRED)*, pp. 10–13, 2013. Article (CrossRef Link)
[36] M. I. Asraf, S. Seppanen, R. Sliz, M. Hamalainen, and C. Pomalaza-Raez, "Implementation issues for wireless medical devices," in *Proc. of Int. Symp. Med. Inf. Commun. Technol.* (ISMICT 2007), 2007.
[37] T. G. Robertazzi, Basics of Computer Networking., Springer, 2012. Article (CrossRef Link)
[38] Y. Chang, C. P. Lee, and J. A. Copeland, "Goodput Optimization in CSMA/CA Wireless Networks," Forth Int. Conf. Braodband Commun. Networks Syst., pp. 880–888, 2007.
[39] M. H. Manshaei and J. Hubaux, "Performance Analysis of the IEEE 802.11 Distributed Coordination Function: Bianchi Model," Mob. Networks, Commun. Syst. Comput. Sci. Div., pp. 1–8, 2007.
[40] C. Song, H. R. Sharif, and P. Mahasukhon, "Evaluating saturation throughput performance of the IEEE 802.11 MAC under fading channels," *2nd Int. Conf. Broadband Networks, BROADNETS 2005*, vol. 2005, pp. 726–731, 2005. Article (CrossRef Link)
[41] H. Zhai, Y. Kwon, and Y. Fang, "Performance analysis of IEEE 802.11 MAC protocols in wireless LANs," *Wirel. Commun.* Mob. Comput., vol. 4, no. 8, pp. 917–931, 2004. Article (CrossRef Link)
[42] D. Xu, T. Sakurai, and H. L. Vu, "An Analytical Model of MAC Access Delay in IEEE 802.11e EDCA," *IEEE Wirel. Commun.* Netw. Conf. WCNC, pp. 1938–1943, 2006.
[43] H. L. Vu and T. Sakurai, "Collision Probability in Saturated IEEE 802.11 Networks," *Aust. Telecommun. Networks Appl. Conf.*, 2006.
[44] M. Heusse, F. Rousseau, G. Berger-sabbatel, and A. Duda, "Performance Anomaly of 802.11b," *INFOCOM 2003. Twenty-Second Annu. Jt. Conf. IEEE Comput. Commun. IEEE* Soc., vol. 2, pp. 836–843, 2003. Article (CrossRef Link)
[45] W. Xiuchao and A. L. Ananda, "Link characteristics estimation for IEEE 802.11 DCF based WLAN," in *Proc. of 29th Annu. IEEE Int. Conf. Local Comput. Networks*, 2004, pp. 302–309, 2004. Article (CrossRef Link)
[46] L. Xie, G. Wei, and H. Wang, "Performance Analysis of IEEE 802.11 DCF in Multi-hop Ad Hoc Networks," in *Proc. of IEEE/ACIS Int. Conf. Comput. Inf.* Sci., pp. 222–227, 2009.
[47] O. Tickoo and B. Sikdar, "Queueing Analysis and Delay Mitigation in IEEE 802.11 Random Access MAC based Wireless Networks," in *Proc. of Int. Conf. Proc. IEEE IN-FOCOM*, Hong Kong, China, pp. 1404–1413, 2004. Article (CrossRef Link)
[48] Y. C. Tay and K. C. Chua, "A Capacity Analysis for the IEEE 802.11 MAC Protocol," *Wirel. Networks*, pp. 159–171, 2001. Article (CrossRef Link)
[49] T. Begin, B. Baynat, I. Guérin, and T. Abreu, "Performance analysis of multi-hop flows in IEEE 802.11 networks: A flexible and accurate modeling framework," *Perform. Eval.*, vol. 96, pp. 12–32, 2016. Article (CrossRef Link)
[50] J. Liu and Z. Niu, "Delay Analysis of IEEE 802.11e EDCA Under Unsaturated Conditions," *IEEE Wirel. Commun. Netw. Conf.*, pp. 430–434, 2007. Article (CrossRef Link)
[51] S. B.-H. Ng Chee-Hock, Fundamentals With Applications in Communication Networks. 2nd Edition. Wiley, 2008.
[52] S. K. Bose, "Priority Operation of The M / G / 1 Queue," Queue, no. 1, pp. 1–11, 2002.

Sajid M. Sheikh holds a PhD degree in Electrical Engineering from Stellenbosch Univeristy, South Africa. He is a registered Member of IEEE and INSTICC. He Sheikh is currently a Senior Lecturer in the Department of Electrical Engineering at the University of Botswana in Gaborone, Botswana. His research interests include scheduling and routing strategies in wireless multi-hop mesh networks, communication networks and systems, mLearning implementations and embedded systems.

Riaan Wolhuter holds a PhD in Electronics from Stellenbosch University, South Africa, where he is a Senior Researcher in the Dept of Electrical and Electronic Eng. He has more than 40 years professional experience in electronic systems in general, but specialises in fixed and mobile telecommunications systems. His experience was obtained in private practice, research and academic environments. He is a Senior Member of both the IEEE and the SA Institute of Electrical Engineers. He also has a keen interest in wildlife photography and visiting the Southern African natural wilderness areas

Herman A. Engelbrecht received his Ph.D. degree in Electronic Engineering from Stellenbosch University, South Africa in 2007. He joined the Department of Electrical and Electronic Engineering in 2004 and is currently a Senior Lecturer in Telecommunication and Signal Processing. He is also one of the directors of the MIH Media Lab, conducting research into distributed systems, specifically gaming systems and massive multiuser virtual environments. Dr Engelbrecht is registered as a PrEng in South Africa, Member of the IEEE, and a Professional Member of the ACM.